Progress In Electromagnetics Research, PIER 45, 45–75, 2004

AN APPROXIMATE SOLUTION FOR SKEW INCIDENCE DIFFRACTION BY AN INTERIOR RIGHT-ANGLED ANISOTROPIC IMPEDANCE WEDGE

G. Manara and P. Nepa

Department of Information Engineering
University of Pisa
Via Diotisalvi 2, I-56126 Pisa, Italy

G. Pelosi and A. Vallecchi

Department of Electronics and Telecommunications
University of Florence
Via S. Marta 3, I-50139 Florence, Italy

Abstract—The scattering by an anisotropic impedance interior right-angled wedge is analyzed when the principal anisotropy directions on the two faces are parallel and perpendicular to the edge. The problem is first approached by directly applying geometrical optics (GO); this allows us to identify the conditions under which the edge diffracted contribution vanishes. For those configurations not satisfying the above conditions, a perturbative technique, based on the Sommerfeld-Maliuzhinets method, is developed to determine an approximate edge diffracted field solution, valid when the normalized surface impedances on the anisotropic faces assume small values. The perturbative corrections to the field are asymptotically evaluated in the context of the Uniform Geometrical Theory of Diffraction (UTD).

1. INTRODUCTION

Electromagnetic scattering from edged anisotropic impedance surfaces is a topic of remarkable interest for a wide class of applications as, for instance, the design of high-frequency antennas [1], polarizing structures [2], and radar calibrated targets [3].

In the framework of a standard ray technique, the geometry of the actual scattering object can be locally approximated by resorting to canonical shapes, whereas its electromagnetic properties can be accounted for by adopting suitable approximate impedance boundary conditions (IBC's) [4]. IBC's constitute a very useful approximation for approaching an extended variety of engineering problems, since they allow to evaluate the material effects avoiding the calculation of the fields within the material itself. However, rigorous solutions for plane wave scattering by non-perfectly conducting wedges illuminated at oblique incidence have been derived only for some specific geometrical and electrical wedge configurations [4, 5]. Indeed, a major difficulty in solving canonical electromagnetic diffraction problems concerning impedance wedges consists in the fact that the IBC's holding on the wedge faces couple the electric and magnetic field components parallel to the edge, which are commonly used as potential functions to express all the other field components. To overcome this problem, the determination of diffraction coefficients for edges in non-perfectly conducting surfaces has been pursued by several approaches, either in a purely numerical way as, for instance, by the method of moments [6] and by the parabolic equation method (PEM), the latter pioneered by Malizhinets [7] and subsequently improved and extended in [8–10], or by resorting to perturbation methods [11–14].

Among unsolved cases, a configuration of great interest is represented by an interior right-angled wedge, characterized by tensor surface impedance faces with their principal anisotropy axes parallel and perpendicular to the edge. It has been shown [15] that, when the tensor surface impedances relevant to the wedge faces satisfy the compatibility relation introduced by Dybdal *et al.* in [16], the exact solution of the above problem can be written in terms of just geometrical optics contributions. It is worth observing that the work in [16] is relevant to the analysis of propagation in a rectangular waveguide with anisotropic impedance walls.

As a preliminary step, we show that the Dybdal compatibility relation [16] can be derived by a GO analysis of the problem, since, as far as it holds, the edge diffracted contribution exactly vanishes. Then, an approximate analytical solution for skew incidence is provided when the edge diffracted contribution does not vanish, no rigorous solution having been presented in the literature so far. This is accomplished by resorting to a perturbation technique based on the Sommerfeld-Maliuzhinets method [17], considering the perfectly conducting case as the unperturbed configuration. A similar approach has been applied in [15], the small parameter in both solutions consisting of the normalized surface impedance, but exploiting the two-dimensional Green's function instead of the Sommerfeld-Maliuzhinets representation. In this paper, Sommerfeld-type approximate integral representations for the longitudinal components of the total field are determined by expanding in the form of a Taylor series the corresponding spectral functions with respect to the normalized surface impedances. All terms up to third order are taken into account, differently from [15] where only terms up to second order are considered. As a result, improved accuracy is achieved at the cost of a slight increase in analytical and computational complexity.

The paper has been organized as follows. The problem is formulated in Section 2, and the conditions under which the edge diffracted contribution vanishes are determined in Section 3 by directly applying GO. Then, in Section 4, suitable approximate integral representations for the longitudinal components of the fields are introduced. The perturbative corrections to the field are asymptotically evaluated in the context of the Uniform Geometrical Theory of Diffraction (UTD) [18] to yield approximate analytical expressions for the edge diffracted field contributions. Finally, samples of numerical results are presented in Section 5 in order to check the accuracy and convergence of the proposed pertubative solution and to discuss its limits of applicability. The results are compared with those obtained by the parabolic equation method [8].

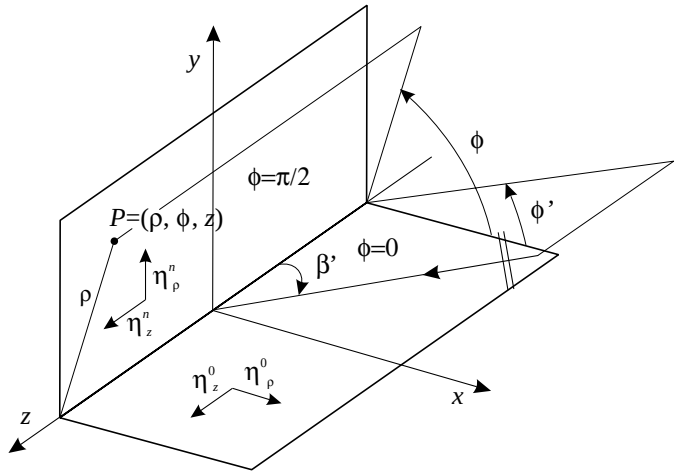

Figure 1. Geometry of the scattering problem.

2. FORMULATION OF THE SCATTERING PROBLEM

The geometry for the scattering problem is depicted in Fig. 1. The anisotropic impedance wedge has its edge along the z-axis of a cylindrical reference frame. The exterior wedge angle is $n\pi$, where $n = 1/2$ for the right-angled wedge case we will refer to. The wedge is illuminated by an arbitrarily polarized plane wave, impinging from a direction determined by the two angles β' and ϕ' ($\beta' = \pi/2$ at normal incidence). A time harmonic dependence $\exp(j\omega t)$ is assumed and suppressed. The longitudinal components of the incident field can be expressed as

$$\begin{bmatrix} E_z^i \\ \zeta H_z^i \end{bmatrix} = \begin{bmatrix} e_z^i \\ h_z^i \end{bmatrix} e^{-jkz\cos\beta'} e^{jk_t\rho\cos(\phi-\phi')}, \tag{1}$$

where k and ζ are the wave number and intrinsic impedance of free space, respectively, $k_t = k\sin\beta'$ is the transverse component of the wave vector and $0 \leqslant \phi' \leqslant \pi/2$. The observation point is located at $P \equiv (\rho, \phi, z)$. Since the electric properties of the wedge are supposed to be independent of z, the scattered field exhibits the same $\exp(-jkz\cos\beta')$ dependence on z as the incident field, that will be understood in the following. Two different anisotropic IBC's hold on the wedge faces; the principal anisotropy axes are assumed to be parallel and perpendicular to the edge so that the IBC's assume the

following form:

$$\begin{bmatrix} E_z \\ \epsilon_{0,n} E_\rho \end{bmatrix} = \begin{bmatrix} \eta_z^{0,n} & 0 \\ 0 & \eta_\rho^{0,n} \end{bmatrix} \begin{bmatrix} -\epsilon_{0,n} \zeta H_\rho \\ \zeta H_z \end{bmatrix}, \quad \phi = 0, n\pi, \tag{2}$$

with $\epsilon_0 = 1$ and $\epsilon_n = -1$. For passive surfaces the elements of the above impedance matrices, normalized to the free-space characteristic impedance, must satisfy the conditions $\Re[\eta_z^{0,n}] \geqslant 0$ and $\Re[\eta_\rho^{0,n}] \geqslant 0$.

The longitudinal components $[E_z, \zeta H_z]$ of the total field, which, as already mentioned, can be used as potential functions to express all the other field components, are solution to the Helmholtz equation $\left(\nabla_t^2 + k_t^2\right)[E_z,\ \zeta H_z] = 0$ and must satisfy the radiation and edge conditions. By expressing the IBC's (2) in terms of $[E_z, \zeta H_z]$, a set of coupled partial differential equations is obtained:

$$\left[\frac{1}{\rho}\frac{\partial}{\partial \phi} \mp \frac{j}{\eta_z^{0,n}} k_t \sin\beta'\right] E_z - \cos\beta' \frac{\partial}{\partial \rho}\left(\zeta H_z\right) = 0, \tag{3a}$$

$$\left[\frac{1}{\rho}\frac{\partial}{\partial \phi} \mp j\eta_\rho^{0,n} k_t \sin\beta'\right] \left(\zeta H_z\right) + \cos\beta' \frac{\partial}{\partial \rho} E_z = 0. \tag{3b}$$

However, when the incidence direction of the plane wave lies on the plane perpendicular to the edge ($\beta' = \pi/2$), the IBC's decouple and the problem reduces to a pair of equivalent scalar impedance wedge problems, whose solution has been given by Maliuzhinets in [17] for a wedge with an arbitrary exterior angle. In the above paper, it is shown that for the geometrical configuration here under analysis the total field coincides with that predicted by the only GO solution; the latter consists of four plane waves representing: *i*) the incident field; *ii*) two plane waves singly reflected by each face of the wedge; *iii*) a doubly reflected plane wave.

3. GEOMETRICAL OPTICS SOLUTION

Let us first discuss the GO solution for the more general oblique incidence case. The longitudinal field components of the electric and magnetic fields can be written as the superposition of the incident field, the field reflected from the face $\phi = 0$, the field reflected from the face $\phi = \pi/2$, and the doubly-reflected field. The latter contribution is made of two terms: *i*) the field first reflected from the face $\phi = 0$ and then from the face $\phi = \pi/2$; *ii*) the field first reflected from the face $\phi = \pi/2$ and then from the face $\phi = 0$. These fields have their own lit regions that are separated by the boundary at $\phi = \phi'$. This is actually the only shadow boundary in the ninety-degrees angular sector here

of interest, and the continuity of the GO solution at this boundary depends on the properties of the double reflection matrix.

In particular, the fields singly-reflected from the faces $\phi = 0,\ \pi/2$ can be expressed as:

$$\begin{bmatrix} E_z^{0,n} \\ \zeta H_z^{0,n} \end{bmatrix} = \overline{\overline{R}}_{0,n} \begin{bmatrix} e_z^i \\ h_z^i \end{bmatrix} e^{j\epsilon_{0,n} k_t \rho \cos(\phi + \phi')}, \tag{4}$$

where the entries of the reflection matrices $\overline{\overline{R}}_{0,n} = \begin{bmatrix} R_{0,n}^{ee} & R_{0,n}^{eh} \\ R_{0,n}^{he} & R_{0,n}^{hh} \end{bmatrix}$ are given by

$$\begin{aligned} R_{0,n}^{ee} &= \left\{ \left[\epsilon_{0,n} \sin(\phi_{0,n}) - \frac{\sin\beta'}{\eta_z^{0,n}} \right] \left[\epsilon_{0,n} \sin(\phi_{0,n}) + \eta_\rho^{0,n} \sin\beta' \right] + \right. \\ &\quad \left. - \cos^2\beta' \cos^2(\phi_{0,n}) \right\} \Big/ \Delta_{0,n}, \\ R_{0,n}^{eh} &= -\cos\beta' \sin(2\phi') \Big/ \Delta_{0,n}, \\ R_{0,n}^{hh} &= \left\{ \left[\frac{\sin\beta'}{\eta_z^{0,n}} + \epsilon_{0,n} \sin(\phi_{0,n}) \right] \left[\epsilon_{0,n} \sin(\phi_{0,n}) - \eta_\rho^{0,n} \sin\beta' \right] + \right. \\ &\quad \left. - \cos^2\beta' \cos^2(\phi_{0,n}) \right\} \Big/ \Delta_{0,n}, \\ R_{0,n}^{he} &= -R_{0,n}^{eh} \end{aligned} \tag{5}$$

and

$$\begin{aligned} \Delta_{0,n} = &\left[\frac{\sin\beta'}{\eta_z^0} + \epsilon_{0,n} \sin(\phi_{0,n}) \right] \left[\epsilon_{0,n} \sin(\phi_{0,n}) + \sin\beta' \eta_\rho^0 \right] \\ &+ \cos^2\beta' \cos^2(\phi_{0,n}). \end{aligned} \tag{6}$$

Moreover, in (5) it has been set

$$\phi_0 = \phi', \quad \phi_n = \phi' - \frac{\pi}{2}. \tag{7}$$

The doubly-reflected field can be written as follows:

$$\begin{bmatrix} E_z^{2r} \\ \zeta H_z^{2r} \end{bmatrix} = \left[U(\phi - \phi') \overline{\overline{R}}_{n0} + U(\phi' - \phi) \overline{\overline{R}}_{0n} \right] \begin{bmatrix} e_z^i \\ h_z^i \end{bmatrix} e^{-jk_t \rho \cos(\phi - \phi')}, \tag{8}$$

where $U(\cdot)$ is the Heaviside unit step function and the double reflection matrices can be expressed in terms of $\overline{\overline{R}}_0$ and $\overline{\overline{R}}_n$ by the following relationships:

$$\overline{\overline{R}}_{0n} = \overline{\overline{R}}_0{}^T \overline{\overline{R}}_n, \quad \overline{\overline{R}}_{n0} = \overline{\overline{R}}_n{}^T \overline{\overline{R}}_0\,, \tag{9}$$

with the apex "T" denoting the transpose of the matrix. It can be shown that the GO solution only exhibits a discontinuity in the cross-polar components of the doubly-reflected field when

$$\overline{\overline{R}}_0{}^T \overline{\overline{R}}_n \neq \overline{\overline{R}}_n{}^T \overline{\overline{R}}_0\,. \tag{10}$$

Indeed, by subtracting the left and the right term in (10) we obtain:

$$\overline{\overline{R}}_0{}^T \overline{\overline{R}}_n - \overline{\overline{R}}_n{}^T \overline{\overline{R}}_0 = \frac{2\delta \cos\beta' \sin(2\phi') \sin^2\beta'}{\eta_z^0 \eta_z^n \Delta_0 \Delta_n} \begin{bmatrix} 0 & -1 \\ 1 & 0 \end{bmatrix}, \tag{11}$$

where

$$\delta = \eta_\rho^0 \eta_z^n + \eta_\rho^n \eta_z^0 - \eta_z^0 \eta_z^n. \tag{12}$$

From (11), it directly follows that the co-polar components of the doubly-reflected field are always continuous. Moreover, it is apparent that the cross-polar components are continuous at normal incidence ($\beta' = \pi/2$) and when $\delta = 0$, that is, when the Dybdal compatibility relation is met [16]. The above condition is apparently satisfied when a face of the wedge is perfectly conducting; this can also be easily verified by directly applying image theory. Moreover, the vanishing of expression (12) is also obtained when: *i)* $\eta_\rho^0 = 0, \eta_z^n = \eta_\rho^n$; *ii)* $\eta_z^0 = \eta_z^n = 0$. As a consequence, it is seen that the asymptotic evaluations of the rigorous spectral solutions proposed in [5] reduce, in the latter cases, to the only GO contributions.

At oblique incidence and when the surface impedances do not satisfy the condition $\delta = 0$, an edge diffracted term is exhibited by the total field; moreover, surface waves may be excited at the edge and propagate along the faces of the wedge. We note that all the GO contributions are continuous, with the exception of the cross-polar component associated with the doubly reflected plane wave, which exhibits a discontinuity at $\phi = \phi'$. This discontinuity is proportional to the parameter δ defined in (12). Consequently, when $\delta \neq 0$ an edge diffracted contribution is needed to compensate for the above discontinuity in the cross-polar component. In the case of a waveguide, we observe that the validity of the Dybdal compatibility condition is required to guarantee the existence of a discrete modal expansion for the field inside the waveguide.

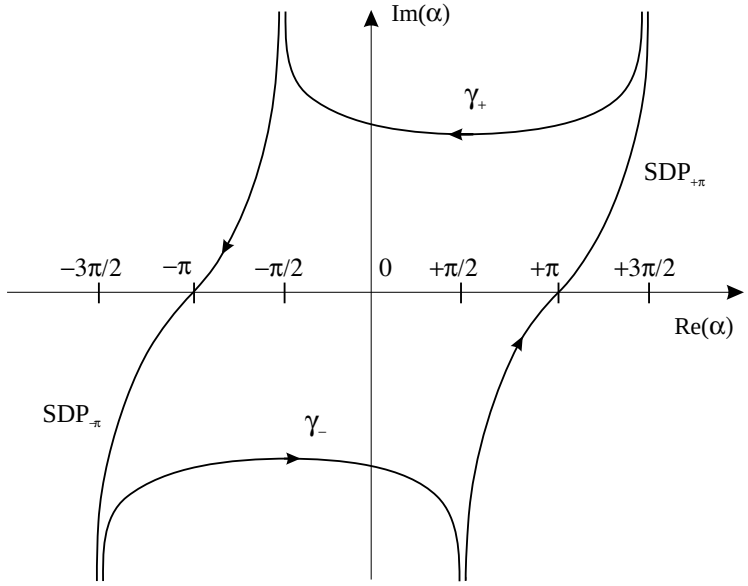

Figure 2. Contours of integration on the complex α-plane.

4. AN APPROXIMATE UTD SOLUTION

A perturbative approach is proposed in this section in combination with the Sommerfeld-Maliuzhinets method [17] to determine suitable spectral representations for the total field, in the presence of an anisotropic impedance interior right-angled wedge. These integral expressions are then asymptotically evaluated in the framework of the UTD.

According to the Maliuzhinets approach [17], $[E_z, \zeta H_z]$ can be expressed in terms of the following spectral representations along the Sommerfeld integration path $\gamma = \gamma^+ + \gamma^-$ (Fig. 2):

$$\begin{bmatrix} E_z \\ \zeta H_z \end{bmatrix} = \frac{1}{2\pi j} \int_\gamma \begin{bmatrix} s_e\left(\alpha + \phi - \dfrac{\pi}{4}\right) \\ s_h\left(\alpha + \phi - \dfrac{\pi}{4}\right) \end{bmatrix} e^{jk_t \rho \cos\alpha} d\alpha. \tag{13}$$

To satisfy the radiation condition, the spectral functions in (13) must be regular in the strip $|\mathrm{Re}(\alpha)| \leq \pi/4$, except for a first order pole at $\alpha = \phi' - \pi/4$ accounting for the incident field. Furthermore, in the same strip, the edge condition requires that $|[s_e(\alpha), s_h(\alpha)] - [s_e(\pm j\infty), s_h(\pm j\infty)]| < \exp[-c\,|\mathrm{Im}(\alpha)|]$, $c > 0$, in the limit for $|\mathrm{Im}(\alpha)| \to \infty$ [19].

When the spectral representations in (13) are inserted into the IBC's in (3), the following set of coupled functional equations is obtained:

$$\left(\eta_z^{0,n}\sin\alpha - \epsilon_{0,n}\sin\beta'\right) s_e\left(\alpha_{0,n}^{+}\right) + \left(\eta_z^{0,n}\sin\alpha + \epsilon_{0,n}\sin\beta'\right) s_e\left(\alpha_{0,n}^{-}\right) = \eta_z^{0,n}\cos\beta'\cos\alpha\left[s_h\left(\alpha_{0,n}^{+}\right) - s_h\left(\alpha_{0,n}^{-}\right)\right], \tag{14a}$$

$$\left(\sin\alpha - \epsilon_{0,n}\eta_\rho^{0,n}\sin\beta'\right) s_h\left(\alpha_{0,n}^{+}\right) + \left(\sin\alpha + \epsilon_{0,n}\eta_\rho^{0,n}\sin\beta'\right) s_h\left(\alpha_{0,n}^{-}\right) = -\cos\beta'\cos\alpha\left[s_e\left(\alpha_{0,n}^{+}\right) - s_e\left(\alpha_{0,n}^{-}\right)\right], \tag{14b}$$

where

$$\alpha_{0,n}^{\pm} = \left(\pm\alpha - \epsilon_{0,n}\frac{\pi}{4}\right). \tag{15}$$

These equations can not be solved rigorously. Nevertheless, in the framework of a perturbative technique, under the hypothesis of small but arbitrary surface impedances so that it can be written

$$\eta_{\rho,z}^{0,n} = \upsilon\xi_{\rho,z}^{0,n}, \tag{16}$$

with $\left|\xi_{\rho,z}^{0,n}\right|$ of order unity and $\upsilon \ll 1$, we can seek for approximate representations of the unknown spectral functions in the form of Taylor series expansions with respect to the parameter υ. Considering only terms up to the third order, we have the following expressions:

$$s_e(\alpha) \simeq s_0^e(\alpha) + \upsilon s_1^e(\alpha) + \upsilon^2 s_2^e(\alpha) + \upsilon^3 s_3^e(\alpha), \tag{17a}$$

$$s_h(\alpha) \simeq s_0^h(\alpha) + \upsilon s_1^h(\alpha) + \upsilon^2 s_2^h(\alpha) + \upsilon^3 s_3^h(\alpha). \tag{17b}$$

By substituting (17) into the functional equations in (14) and equating the coefficients of like powers of υ, a set of recursive decoupled functional equations is obtained for $[s_i^e(\alpha), s_i^h(\alpha)]$, with $i = 0, 1, 2, 3$ [13, 14]:

$$s_i^e\left(\alpha_{0,n}^{+}\right) - s_i^e\left(\alpha_{0,n}^{-}\right) = \epsilon_{0,n}\xi_z^{0,n}\left\{\frac{\sin\alpha}{\sin\beta'}\left[s_{i-1}^e\left(\alpha_{0,n}^{+}\right) + s_{i-1}^e\left(\alpha_{0,n}^{-}\right)\right] + -\frac{\cos\alpha}{\tan\beta'}\left[s_{i-1}^h\left(\alpha_{0,n}^{+}\right) - s_{i-1}^h\left(\alpha_{0,n}^{-}\right)\right]\right\}, \tag{18a}$$

$$s_i^h\left(\alpha_{0,n}^+\right)+s_i^h\left(\alpha_{0,n}^-\right)=-\epsilon_{0,n}\left\{\xi_z^{0,n}\frac{\cos\alpha}{\tan\beta'}\left[s_{i-1}^e\left(\alpha_{0,n}^+\right)+s_{i-1}^e\left(\alpha_{0,n}^-\right)\right]+\right.$$
$$\left.-\left[\xi_\rho^{0,n}\frac{\sin\beta'}{\sin\alpha}+\xi_z^{0,n}\frac{\cos\beta'\cos\alpha}{\tan\beta'\tan\alpha}\right]\left[s_{i-1}^h\left(\alpha_{0,n}^+\right)-s_{i-1}^h\left(\alpha_{0,n}^-\right)\right]\right\}. \tag{18b}$$

where $s_{-1}^{e,h}(\alpha)=0$. In particular, $[s_0^e(\alpha),s_0^h(\alpha)]$ are the spectral functions relevant to the diffraction of a plane wave impinging on a perfectly conducting wedge with TM_z and TE_z polarizations, respectively, and are known in closed form [20]:

$$s_0^e(\alpha)=\frac{2\,e_z^i\sin(2\phi')}{\sin(2\alpha)+\cos(2\phi')},\quad s_0^h(\alpha)=\frac{2\,h_z^i\cos(2\alpha)}{\sin(2\alpha)+\cos(2\phi')}. \tag{19}$$

It is noted that in this case the total field reduces to the GO field contributions only. Moreover, $[s_1^e(\alpha),s_1^h(\alpha)]$ and $[s_2^e(\alpha),s_2^h(\alpha)]$ must satisfy inhomogeneous functional equations of the Maliuzhinets type whose solutions can be derived in closed form through the application of the modified Fourier transform introduced in [21]. Explicit expressions for $[s_1^e(\alpha),s_1^h(\alpha)]$ and $[s_2^e(\alpha),s_2^h(\alpha)]$ are given in Appendices A and B, respectively. As far as $s_3^e(\alpha)$ and $s_3^h(\alpha)$ are concerned, closed form expressions can not be determined anymore; suitable integral representations have been obtained by following a procedure similar to that used in [13] and [14]. Indeed, the third-order terms contain special integral functions that have the form of Tuzhilin integrals [22]. However, the expressions for the third order terms are very complicated and only their asymptotic approximations will be provided in this paper. Attention is called to the fact that the higher order terms of the expansion (17) are related to the derivatives of the scattered field with respect to υ and not directly to the field. Thus, they are not expected to individually fulfil the requirement descending from the edge condition that applies to the spectra and, hence, to the full series expansion (17) for $|\mathrm{Im}(\alpha)|\to\infty$. Indeed, by truncating the above expansion, the boundedness of the Sommerfeld transforms might become questionable for some value of the parameter υ and, in turn, the proper behaviour of the field in the vicinity of the edge could not be reliably predicted. Nevertheless, this is not an issue since this work aims at deriving analytical approximated expressions to accurately estimate the electromagnetic field scattered by a right angled anisotropic impedance wedge in the far zone. Furthermore, it is worth noting that the higher order spectral functions are regular in the strip $|\mathrm{Re}(\alpha)|\leqslant\pi/4$, since the pole singularities providing the contribution of the incident field have been already accounted for in $[s_0^e(\alpha),s_0^h(\alpha)]$.

Introducing (17) in (13), the longitudinal components of the total field $[E_z, \zeta H_z]$ are expressed in the form of a summation of Sommerfeld integrals as

$$\begin{bmatrix} E_z \\ \zeta H_z \end{bmatrix} \simeq \sum_{i=0}^{3} \frac{\upsilon^i}{2\pi j} \int_\gamma \begin{bmatrix} s_i^e\left(\alpha+\phi-\frac{\pi}{4}\right) \\ s_i^h\left(\alpha+\phi-\frac{\pi}{4}\right) \end{bmatrix} e^{jk_t\rho\cos\alpha} d\alpha. \tag{20}$$

In particular, by applying the residue theorem, all the above integral representations for the total field along the Sommerfeld integration contour γ are reduced to the contributions of two integrals, defined along the steepest descent paths $\mathrm{SDP}_{\pm\pi}$ through the saddle points at $\pm\pi$ (see Fig. 2), and that of the residues of the poles of $[s_i^e(\alpha), s_i^h(\alpha)]$, $i = 0, 1, 2, 3$, which can be captured in the contour deformation process:

$$\begin{aligned} \begin{bmatrix} E_z \\ \zeta H_z \end{bmatrix} = {} & \sum_{i=0}^{3} \upsilon^i \sum_j \mathrm{Res}\left\{ \begin{bmatrix} s_i^e(\alpha) \\ s_i^h(\alpha) \end{bmatrix}, \alpha = \alpha_{p_{ij}} \right\} e^{jk_t\rho\cos\left(\alpha_{p_{ij}}-\phi+\pi/4\right)} + \\ & - \frac{1}{2\pi j} \sum_{i=1}^{3} \upsilon^i \int_{\mathrm{SDP}_{\pm\pi}} \begin{bmatrix} s_i^e\left(\alpha+\phi-\frac{\pi}{4}\right) \\ s_i^h\left(\alpha+\phi-\frac{\pi}{4}\right) \end{bmatrix} e^{jk_t\rho\cos\alpha} d\alpha. \end{aligned} \tag{21}$$

The asymptotic evaluation of the higher order contributions to the field will be discussed in detail in the following.

4.1. Residue Contributions

The spectral functions $\left[s_i^e(\alpha), s_i^h(\alpha)\right]$ exhibit first-order pole singularities of geometrical type whose residues provide the corrections to the singly and doubly reflected field contributions. The locations of these geometrical poles on the complex α-plane are:

$$\begin{aligned} &\alpha = \alpha_0^{go} = -\phi - \phi', && \alpha = \alpha_n^{go} = \pi - \phi - \phi', \\ &\alpha = \alpha_{0n}^{go} = -\pi - \phi + \phi', && \alpha = \alpha_{n0}^{go} = \pi - \phi + \phi'. \end{aligned} \tag{22}$$

The poles at α_0^{go} and α_n^{go}, whose residues provide the corrections to the field reflected from the face $\phi = 0$ and $\phi = \pi/2$, respectively, lie in the strip $|\mathrm{Re}(\alpha)| < \pi$ and, therefore, are always captured in the contour deformation process. Conversely, the poles at α_{0n}^{go} and α_{n0}^{go} can cross the SDP's for $\phi = \phi'$ at the saddle points $-\pi$ and π, respectively; the corresponding residues yield the corrections to the doubly reflected field. Thus, the latter residues must be included in the asymptotic solution only when $\phi < \phi'$ and $\phi > \phi'$, respectively.

Since the locations of the poles of the spectral functions are the same regardless of their order, the residue contributions can be written in general as:

$$\mathrm{Res}\left\{\begin{bmatrix} s_i^e\left(\alpha+\phi-\frac{\pi}{4}\right) \\ s_i^h\left(\alpha+\phi-\frac{\pi}{4}\right)\end{bmatrix} e^{jk_t\rho\cos\alpha}, \alpha=\alpha_t^{go}\right\} = \begin{bmatrix} r_t^{e\,i} \\ r_t^{h\,i}\end{bmatrix} e^{jk_t\rho\cos\left(\alpha_t^{go}\right)}, \tag{23}$$

where $i = 1, 2, 3$ and $r_t^{e,\,h\,i}$ represents the residue of $s_i^e(\alpha)$ or $s_i^h(\alpha)$ associated with the pole α_t^{go}, $t = 0, n, 0n, n0$. The contributions in (23) correspond to the i-th order terms in a series expansion of the GO solution with respect to v. More precisely, the residue expressions in (23) are proportional to the i-th derivatives with respect to v of the singly and doubly-reflected electric and magnetic fields.

4.1.1. First-Order Residue Contributions

Explicit expressions for the residue of the first-order corrections are:

$$\begin{aligned} r_0^{e1} &= \frac{2\xi_z^0}{\sin\beta'}\left(e_z^i\sin\phi' - h_z^i\cos\beta'\cos\phi'\right), \\ r_n^{e1} &= \frac{2\xi_z^n}{\sin\beta'}\left(e_z^i\cos\phi' + h_z^i\cos\beta'\sin\phi'\right), \\ r_{0n}^{e1} &= r_{n0}^{e1} = -\left(r_0^{e1}+r_n^{e1}\right), \end{aligned} \tag{24}$$

and

$$\begin{aligned} r_0^{h1} &= 2\xi_z^0\cos\phi'\cot\beta'\ e_z^i - 2K_0\left(\phi_0\right)h_z^i, \\ r_n^{h1} &= -2\xi_z^n\sin\phi'\cot\beta' e_z^i - 2K_n\left(\phi_n\right)h_z^i, \\ r_{0n}^{h1} &= r_{n0}^{h1} = r_0^{h1} + r_n^{h1}. \end{aligned} \tag{25}$$

In (25)

$$K_{0,n}(\alpha) = \frac{\epsilon_{0,n}}{\sin\alpha}\left(\xi_\rho^{0,n}\sin\beta' + \xi_z^{0,n}\cos\beta'\cot\beta'\cos^2\alpha\right), \tag{26}$$

whereas $\phi_{0,n}$ have been defined in (7). These corrections behave continuously at the doubly reflected field shadow boundary ($\phi = \phi'$); hence, it is expected that the corresponding spectral representations do not provide any diffracted field contribution.

4.1.2. Second-Order Residue Contributions

As far as the second-order correction spectral functions are concerned, the residue expressions can be written as follows:

$$\begin{aligned} r_0^{e2} &= -\frac{\overline{L}_0}{4\cos\phi'}, \\ r_n^{e2} &= -\frac{\overline{L}_n}{4\sin\phi'}, \\ r_{0n}^{e2} &= -\left(r_0^{e2}+r_n^{e2}\right)+\frac{\widehat{L}_0}{\cos\phi'}, \\ r_{n0}^{e2} &= -\left(r_0^{e2}+r_n^{e2}\right)+\frac{\widehat{L}_n}{\sin\phi'}, \end{aligned} \tag{27}$$

and

$$\begin{aligned} r_0^{h2} &= \frac{\overline{M}_0}{4\sin\phi'}, \\ r_n^{h2} &= -\frac{\overline{M}_n}{4\cos\phi'}, \\ r_{0n}^{h2} &= r_0^{h2}+r_n^{h2}+\frac{\widehat{M}_0}{\sin\phi'}, \\ r_{n0}^{h2} &= r_0^{h2}+r_n^{h2}-\frac{\widehat{M}_n}{\cos\phi'}. \end{aligned} \tag{28}$$

The constants appearing in (27) and (28) are defined by

$$\begin{aligned} \overline{L}_{0,n} &= L_{0,n}^1\sin^2(\phi_{0,n})+L_{0,n}^2\sin^2\left(2\phi'\right) \\ &\quad + L_{0,n}^3\cos^2(\phi_{0,n})+L_{0,n}^4\cos^4(\phi_{0,n}), \\ \widehat{L}_{0,n} &= \left[L_{0,n}^5+L_{0,n}^6\sin^2(\phi_{0,n})\right]\cos^2(\phi_{0,n}), \\ \overline{M}_{0,n} &= M_{0,n}^1+M_{0,n}^2\cos^2(\phi_{0,n})+M_{0,n}^3\cos^4(\phi_{0,n}) \\ &\quad + M_{0,n}^4\sin^2(\phi_{0,n})+M_{0,n}^5\sin^2\left(2\phi'\right), \\ \widehat{M}_{0,n} &= M_{0,n}^6+M_{0,n}^7\sin^2(\phi_{0,n})+M_n^8\sin^2\left(2\phi'\right), \end{aligned} \tag{29}$$

while $L_{0,n}^m$, $m=1,2,\ldots 6$, $M_{0,n}^l$, $l=1,2,\ldots 8$ have been introduced in Appendix B (Eqs. (B3), (B6)). It is easily noted that the residues in (27) and (28) may behave discontinuously at the shadow boundary of the doubly reflected field ($\phi=\phi'$). These discontinuities are compensated by edge diffracted field contributions.

4.1.3. Third-Order Residue Contributions

Even though the third-order terms contain special integral functions, their residues associated with the geometrical poles can be derived in closed form:

$$
\begin{aligned}
r_0^{e3} &= \frac{\xi_z^0}{4\sin\beta'}\left(\frac{\overline{L}_0}{\cot\phi'} - \frac{\cos\beta'\overline{M}_0}{\tan\phi'}\right),\\
r_n^{e3} &= -\frac{\xi_z^n}{4\sin\beta'}\left(\frac{\overline{L}_n}{\tan\phi'} + \frac{\cos\beta'\overline{M}_n}{\cot\phi'}\right),\\
r_{0n}^{e3} &= -\left(r_0^{e3}+r_n^{e3}\right)+\frac{\xi_z^0}{2\sin\beta'}\left[\overline{L}_n-\cos\beta'\left(\overline{M}_n-\frac{2\widehat{M}_0}{\tan\phi'}\right)-\frac{2\widehat{L}_0}{\cot\phi'}\right],\\
r_{n0}^{e3} &= -\left(r_0^{e3}+r_n^{e3}\right)-\frac{\xi_z^n}{2\sin\beta'}\left[\overline{L}_0+\cos\beta'\left(\overline{M}_0-\frac{2\widehat{M}_n}{\cot\phi'}\right)+\frac{2\widehat{L}_n}{\tan\phi'}\right],
\end{aligned}
\tag{30}
$$

and

$$
\begin{aligned}
r_0^{h3} &= \frac{\xi_z^0\overline{L}_0}{4\tan\beta'} - \frac{K_0\left(\phi_0\right)\overline{M}_0}{4\sin\phi'},\\
r_n^{h3} &= \frac{\xi_z^n\overline{L}_n}{4\tan\beta'} - \frac{K_n\left(\phi_n\right)\overline{M}_n}{4\cos\phi'},\\
r_{0n}^{h3} &= r_0^{h3}+r_n^{h3}-\frac{\xi_z^0\cot\beta'}{2\tan\phi'}\left(\overline{L}_n-\frac{2\widehat{L}_0}{\cot\phi'}\right)+\frac{K_0(\phi_0)}{2\cos\phi'}\left(\overline{M}_n-\frac{2\widehat{M}_0}{\tan\phi'}\right),\\
r_{n0}^{h3} &= r_0^{h3}+r_n^{h3}-\frac{\xi_z^n\cot\beta'}{2\cot\phi'}\left(\overline{L}_0+\frac{2\widehat{L}_n}{\tan\phi'}\right)-\frac{K_n(\phi_n)}{2\sin\phi'}\left(\overline{M}_0-\frac{2\widehat{M}_n}{\cot\phi'}\right).
\end{aligned}
\tag{31}
$$

Again, third-order term residues are associated with the contributions of three plane waves of which that one contributing to the doubly-reflected field may be discontinuous at $\phi = \phi'$. An edge diffracted field contribution that compensates for such discontinuity will be derived hereinafter.

4.2. Contributions of the SDP Integrals

The integrals along the $\mathrm{SDP}_{\pm\pi}$ give the contributions of the edge diffracted field. Their asymptotic evaluation in the framework of UTD [18] yields a uniform solution for the field that is smooth and continuous at the shadow boundary of the GO fields.

4.2.1. First-Order Diffracted Field Contributions

The first-order edge diffracted field contributions vanish, as expected, since the integrands of the $\mathrm{SDP}_{\pm\pi}$ integrals through the saddle points at $\alpha = \pi$ and $\alpha = -\pi$ (Fig. 2) are periodic, with period 2π. Thus, only the residues of the GO pole singularities contribute to the field.

4.2.2. Second-Order Diffracted Field Contributions

Conversely, the asymptotic evaluations of $s_2^e(\alpha)$ and $s_2^h(\alpha)$ also provide diffracted field contributions, which compensate for the discontinuities of the second-order terms in the series expansion of the GO solution. As a matter of fact, the terms $\widehat{s}_2^{\,e}(\alpha)$ and $\widehat{s}_2^{\,h}(\alpha)$ in Eq. (B1), unlike $\overline{s}_2^{\,e}(\alpha)$ and $\overline{s}_2^{\,h}(\alpha)$ (see (B4) and (B7) for the detailed expressions), are no more periodic and, as a result, non-vanishing terms arise from the $\mathrm{SDP}_{\pm\pi}$ integrals. Uniform asymptotic expressions for the second-order correction edge diffracted field contributions are:

$$\begin{bmatrix} E_z^{2d} \\ \zeta H_z^{2d} \end{bmatrix} = \frac{e^{-j\left(k_t\rho+\frac{\pi}{4}\right)}}{\sqrt{2\pi k_t\rho}} \left(\xi_\rho^0\,\xi_z^n + \xi_z^0\,\xi_\rho^n - \xi_z^0\,\xi_z^n\right) \begin{bmatrix} h_z^i \\ -e_z^i \end{bmatrix} \cdot \frac{8\cos\beta'\sin(2\phi')\,F\left(\sqrt{k_t\rho\,[1-\cos(\phi-\phi')]}\right)}{\cos(2\phi)-\cos(2\phi')}\,\upsilon^2, \tag{32}$$

where $F(\cdot)$ is the UTD transition function [18]. They compensate for the above mentioned discontinuites, however vanishing at normal incidence and when the Dybdal compatibility condition is satisfied. It is worth noting that (32) only contribute to the cross-polar components of the field, as expected.

4.2.3. Third-Order Diffracted Field Contributions

As far as $s_3^e(\alpha)$ and $s_3^h(\alpha)$ are concerned, suitable integral representations have been determined by applying a procedure similar to that used in [13, 14]. The corresponding edge diffracted field contributions are derived by asimptotically evaluating the $\mathrm{SDP}_{\pm\pi}$ integrals to achieve the following uniform expressions:

$$\begin{bmatrix} E_z^{3d} \\ \zeta H_z^{3d} \end{bmatrix} = \frac{e^{-j\left(k_t\rho+\frac{\pi}{4}\right)}}{\sqrt{2\pi k_t\rho}} \begin{bmatrix} \overline{s}_3^{\,e}\left(-\pi+\phi-\frac{\pi}{4}\right) + \overline{s}_3^{\,e}\left(\pi+\phi-\frac{\pi}{4}\right) \\ -\overline{s}_3^{\,h}\left(-\pi+\phi-\frac{\pi}{4}\right) - \overline{s}_3^{\,h}\left(\pi+\phi-\frac{\pi}{4}\right) \end{bmatrix} \cdot \frac{2\,F\left(\sqrt{k_t\rho\,[1-\cos(\phi-\phi')]}\right)}{\cos(2\phi)-\cos(2\phi')}\,\upsilon^3. \tag{33}$$

The functions $\overline{s}_3^e(\alpha)$ and $\overline{s}_3^h(\alpha)$ consist of the terms from the third-order correction spectral functions that are not periodic and can be written in the form:

$$\overline{s}_3^e(\alpha) = w_0^e(\alpha)\cos\phi' + w_n^e(\alpha)\sin\phi' + \widehat{s}_3^e(\alpha), \tag{34a}$$

$$\overline{s}_3^h(\alpha) = w_0^h(\alpha)\cos\phi' + w_n^h(\alpha)\sin\phi' + \widehat{s}_3^h(\alpha). \tag{34b}$$

In particular, for $w_{0,n}^e(\alpha)$ we have

$$\begin{aligned} w_{0,n}^e(\alpha) = \frac{1}{2}\Big[\overline{P}_{0,n}^1\sin^2\Big(\alpha_{0,n}^+\Big) + \overline{P}_{0,n}^2\cos^2(2\alpha) + \overline{P}_{0,n}^3 + \overline{P}_{0,n}^4\cos^2\Big(\alpha_{0,n}^+\Big) \\ + \overline{P}_{0,n}^5\cos^4\Big(\alpha_{0,n}^+\Big) + \overline{P}_{0,n}^6\sin^2\Big(\alpha_{0,n}^+\Big)\cos^2\Big(\alpha_{0,n}^+\Big)\Big]\sin\Big(2\alpha_{0,n}^+\Big), \end{aligned} \tag{35}$$

where it has been set

$$\begin{aligned} &\overline{P}_{0,n}^1 = P_{0,n}^1 + P_{0,n}^8 + P_{0,n}^{13}, \quad &&\overline{P}_{0,n}^2 = P_{0,n}^2 + P_{0,n}^9 + P_{0,n}^{14}, \\ &\overline{P}_{0,n}^3 = P_{0,n}^5 + P_{0,n}^{12}, &&\overline{P}_{0,n}^4 = P_{0,n}^3 + P_{0,n}^6 + P_{0,n}^{10}, \\ &\overline{P}_{0,n}^5 = P_{0,n}^4 + P_{0,n}^7, &&\overline{P}_{0,n}^6 = P_{0,n}^{11}, \end{aligned} \tag{36}$$

and

$$P_{0,n}^i = \begin{cases} -\dfrac{\xi_z^{0,n}L_{0,n}^i}{2\sin\beta'\cos(\phi_{0,n})}, & i = 1,2,\ldots 4, \\ -\dfrac{\xi_z^{0,n}\cos\beta' M_{0,n}^{i-4}}{2\sin\beta'\cos(\phi_{0,n})}, & i = 5,6,\ldots 9, \\ -\dfrac{\xi_z^{0,n}L_{0,n}^{i-5}}{\sin\beta'\cos(\phi_{0,n})}, & i = 10,11, \\ -\dfrac{\xi_z^{0,n}\cos\beta' M_{0,n}^{i-6}}{\sin\beta'\cos(\phi_{0,n})}, & i = 12,13,14. \end{cases} \tag{37}$$

Analogously, the function $w_{0,n}^h(\alpha)$ can be represented as follows

$$\begin{aligned} w_{0,n}^h(\alpha) = \overline{Q}_{0,n}^1\sin^4\Big(\alpha_{0,n}^+\Big) + \overline{Q}_{0,n}^2 + \overline{Q}_{0,n}^3\sin^2\Big(\alpha_{0,n}^+\Big)\cos^2(2\alpha) + \sin^2\Big(\alpha_{0,n}^+\Big) \\ \cdot\Big[\overline{Q}_{0,n}^4\cos^4\Big(\alpha_{0,n}^+\Big) + \overline{Q}_{0,n}^5 + \overline{Q}_{0,n}^7\cos^2\Big(\alpha_{0,n}^+\Big)\Big] + \overline{Q}_{0,n}^6\cos^4\Big(\alpha_{0,n}^+\Big), \end{aligned} \tag{38}$$

with

$$\begin{aligned}
&\overline{Q}^1_{0,n} = Q^1_{0,n} + Q^{13}_{0,n} + Q^{21}_{0,n}, && \overline{Q}^2_{0,n} = Q^5_{0,n} + Q^6_{0,n} + Q^{17}_{0,n},\\
&\overline{Q}^3_{0,n} = Q^2_{0,n} + Q^{14}_{0,n} + \tfrac{1}{4}Q^{16}_{0,n} + Q^{22}_{0,n}, && \overline{Q}^4_{0,n} = Q^4_{0,n} + Q^{12}_{0,n},\\
&\overline{Q}^5_{0,n} = Q^8_{0,n} - Q^6_{0,n} + Q^{10}_{0,n} + Q^{18}_{0,n} + Q^{20}_{0,n}, && \overline{Q}^6_{0,n} = Q^7_{0,n},\\
&\overline{Q}^7_{0,n} = Q^3_{0,n} + 4Q^9_{0,n} + Q^{11}_{0,n} + Q^{15}_{0,n} + 4Q^{19}_{0,n},
\end{aligned} \tag{39}$$

$$Q^i_{0,n} = \begin{cases}
\dfrac{\xi_z^{0,n}\cot\beta' L^i_{0,n}}{2\cos(\phi_{0,n})}, & i = 1, 2, \ldots 4,\\
\dfrac{\xi_\rho^{0,n}\sin\beta' M^{i-4}_{0,n}}{2\cos(\phi_{0,n})}, & i = 5, 6, \ldots 9,\\
\dfrac{\xi_z^{0,n}\cos\beta'\cot\beta' M^{i-9}_{0,n}}{2\cos(\phi_{0,n})}, & i = 10, 11, \ldots 14,\\
\dfrac{\xi_z^{0,n}\cot\beta' L^{i-10}_{0,n}}{\cos(\phi_{0,n})}, & i = 15, 16,\\
\dfrac{\xi_\rho^{0,n}\sin\beta' M^{i-11}_{0,n}}{\cos(\phi_{0,n})}, & i = 17, 18, 19,\\
\dfrac{\xi_z^{0,n}\cos\beta'\cot\beta' M^{i-14}_{0,n}}{\cos(\phi_{0,n})}, & i = 20, 21, 22.
\end{cases} \tag{40}$$

Moreover, the functions $\widehat{s}^e_3(\alpha)$ and $\widehat{s}^h_3(\alpha)$ in (34) satisfy the following inhomogeneous functional equations:

$$\widehat{s}^e_3\left(\alpha^+_{0,n}\right) - \widehat{s}^e_3\left(\alpha^-_{0,n}\right) = \widehat{H}^e_{0,n}(\alpha), \tag{41a}$$

$$\widehat{s}^h_3\left(\alpha^+_{0,n}\right) + \widehat{s}^h_3\left(\alpha^-_{0,n}\right) = \widehat{H}^h_{0,n}(\alpha). \tag{41b}$$

In (41)

$$\widehat{H}^e_{0,n}(\alpha) = \frac{4\xi_z^{0,n}\alpha\cos\alpha H^e_{0,n}(\alpha)}{\pi\sin\beta'\left[\cos(2\alpha) - \epsilon_{0,n}\cos(2\phi')\right]}, \tag{42a}$$

$$\widehat{H}^h_{0,n}(\alpha) = \frac{4\alpha H^h_{0,n}(\alpha)}{\pi\left[\cos(2\alpha) - \epsilon_{0,n}\cos(2\phi')\right]}, \tag{42b}$$

and

$$\begin{aligned} H^e_{0,n}(\alpha) = \cos(\phi_{0,n}) \{ & \sin^2\alpha \left(L^5_{0,n} + L^6_{0,n} \sin^2\alpha \right) + \\ & - \cos\beta' \left[M^6_{0,n} + M^7_{0,n} \sin^2\alpha + M^8_{0,n} \sin^2(2\alpha) \right] \} \\ & + \sin(\phi_{0,n}) \{ \sin^2\alpha \left(L^5_{n,0} + L^6_{n,0} \cos^2\alpha \right) \\ & + \cos\beta' \left[M^6_{n,0} + M^7_{n,0} \cos^2\alpha + M^8_{n,0} \sin^2(2\alpha) \right] \}, \end{aligned} \tag{43a}$$

$$\begin{aligned} H^h_{0,n}(\alpha) = {} & \xi^{0,n}_z \cot\beta' \left[-\cos(\phi_{0,n}) \left(L^5_{0,n} + L^6_{0,n} \sin^2\alpha \right) \right. \\ & \left. + \sin(\phi_{0,n}) \left(L^5_{n,0} + L^6_{n,0} \cos^2\alpha \right) \right] \sin\alpha \cos^2\alpha + K_{0,n}(\alpha) \\ & \cdot \{ \cos(\phi_{0,n}) \left[M^6_{0,n} + M^7_{0,n} \sin^2\alpha + M^8_{0,n} \sin^2(2\alpha) \right] \\ & + \sin(\phi_{0,n}) \left[M^6_{n,0} + M^7_{n,0} \cos^2\alpha + M^8_{n,0} \sin^2(2\alpha) \right] \}. \end{aligned} \tag{43b}$$

The solution of (41) has been given by Tuzhilin in [22], in the form of special integral functions, with the integrals defined along the imaginary axis of the complex plane. It can be written as:

$$\widehat{s}^e_3(\alpha) = \sigma^e_0(\alpha) + \sigma^e_n(\alpha) \tag{44a}$$

$$\widehat{s}^h_3(\alpha) = \sigma^h_0(\alpha) + \sigma^h_n(\alpha) \tag{44b}$$

where

$$\begin{bmatrix} \sigma^e_{0,n}(\alpha) \\ \sigma^h_{0,n}(\alpha) \end{bmatrix} = \frac{1}{2\pi j} \int_{-j\infty}^{+j\infty} \begin{bmatrix} \widehat{H}^e_{0,n}(\tau) \\ \widehat{H}^h_{0,n}(\tau) \end{bmatrix} \tan\left(\alpha - \epsilon_{0,n} \frac{\pi}{4} - \tau \right) d\tau. \tag{45}$$

The previous definitions for $\left[\sigma^e_0(\alpha), \sigma^h_0(\alpha)\right]$ and $\left[\sigma^e_n(\alpha), \sigma^h_n(\alpha)\right]$ are valid in the strip $-\pi/4 < \mathrm{Re}(\alpha) < 3\pi/4$ and $-3\pi/4 < \mathrm{Re}(\alpha) < \pi/4$, respectively. Outside these regions an analytic continuation is required [22], which is based on the functional equations in (41).

It can be shown that $\widehat{H}^e_{0,n}(\tau)$ and $\widehat{H}^h_{0,n}(\tau)$ are odd functions and that their amplitude reduces to zero exponentially when $|\mathrm{Im}(\tau)| \to \infty$. This renders the integrals in (45) rapidly convergent.

Finally, we observe that all the higher order terms can in principle be reconstructed by exploiting the recursive functional equation in (4). However, their expressions are very complicated and will not be provided herein. Anyway, it is worth noting that including terms up to third-order in the perturbative solution is in general sufficient to obtain a good accuracy. A set of numerical results is reported in the next section to confirm the accuracy of the proposed perturbative solution.

5. NUMERICAL RESULTS

Samples of numerical results are presented in this section in order to validate the proposed technique and to discuss its limits of applicability. As a first step, the convergence of this approximate solution has been checked through numerical comparisons with the results obtained by applying the exact GO solution for the co-polar and cross-polar components of the field when the Dybdal compatibility relationship is satisfied, that is, when $\delta = 0$. These preliminary results, which are not reported herein, show that the accuracy of the approximate predictions is progressively augmented by the introduction of the second- and third-order terms, thereby testifying for the consistency of the method. Other comparisons with data obtained by resorting to a numerical solution determined by the parabolic equation method [8] are shown. It is worth noting that, in contrast to numerical solutions, the pertubative approach (PA) proposed in this paper can provide explicit analytic diffraction coefficients, even though under the assumption of small anisotropic impedances. In all the examples presented, the field is calculated at a constant distance from the edge ($k_t\rho = 5$) and is plotted versus the observation angle ϕ.

Comparisons between data relevant to the amplitude of the cross-polar component of the total field, calculated either by the GO solution (continuous lines) or by this approximate method (dashed lines) including corrections up to the third-order, are presented in Fig. 3. The incident plane wave is TE_z polarized ($e_z^i = 0$, $h_z^i = 1$) and impinges on the edge from $\beta' = 60°$, $\phi' = 60°$. Several curves corresponding to different decreasing magnitudes of the impedances on the $\phi = 0$ face of the wedge have been plotted. The face $\phi = \pi/2$ is anisotropic, with $\xi_z^n = (1 + j)/2$, $\xi_\rho^n = (1 + j)/4j$, $\upsilon = 0.2$. It can be noted that the cross-polar longitudinal component significantly depends on the zero-face impedances. In particular, when $\xi_z^0 = j$, $\xi_\rho^0 = j/2$ or $\xi_z^0 = \xi_\rho^0 = 0$, the Dybdal relationship is met and the exact solution reduces to the GO contributions only. A good agreement is observed between the results obtained by the GO and this approximate solution. Conversely, when $\xi_z^0 = \xi_\rho^0 = j/2$ or $\xi_z^0 = j/4$ and $\xi_\rho^0 = j/2$, it results that δ is not equal to zero and a discontinuity arises in the cross-polar component of the GO field at $\phi = \phi'$. The edge diffracted contribution that is needed to compensate for this discontinuity is accurately estimated by the proposed approximate solution, which is everywhere continuous and smoothly reduces to the GO results far from $\phi = \phi'$. Concerning the co-polar longitudinal component, the results obtained by the GO solution and by this approximate solution overlap for every analyzed configuration and are slightly affected by

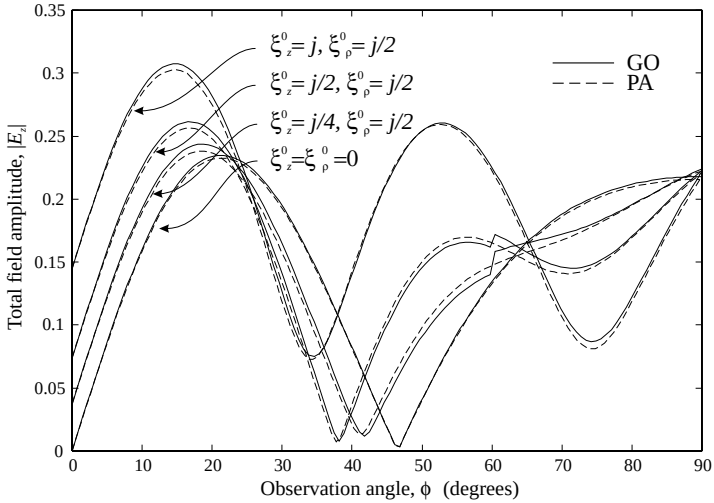

Figure 3. Cross-polar component of the total field (E_z) in the presence of an interior right angled anisotropic impedance wedge with $\xi_z^n = (1+j)/2$, $\xi_\rho^n = (1+j)/4j$ and $\upsilon = 0.2$. The zero-face impedances assume a set of values with decreasing magnitude. The wedge is illuminated by a TE_z polarized ($e_z^i = 0$, $h_z^i = 1$) plane wave impinging from $\beta' = 60°$, $\phi' = 60°$. This approximate solution including up to the third-order correction: dashed line; GO solution: continuous line.

the changes in the zero-face impedance values; the corresponding plots are omitted.

Another example is shown in Fig. 4. Here some curves for the cross-polar longitudinal component of the total field (ζH_z) in the presence of an anisotropic impedance right-angled wedge, with $\xi_z^0 = j/2$, $\xi_\rho^0 = j$, $\xi_z^n = (1+j)/2$, $\xi_\rho^n = j$ and $\upsilon = 0.1$, are plotted. The wedge is illuminated by a TM_z polarized plane wave ($e_z^i = 1$, $h_z^i = 0$), impinging on the edge from a set of directions identified by $\phi' = 45°$ and $\beta' = 45, 60, 75°$. The fields calculated through this perturbative approach (dashed line) including up to the third-order correction are compared with those obtained by the GO solution (continuous lines). Again, the plots for the cross-polar component apparently show that the approximate procedure allow to obtain an appropriate description of the field even in the most general case when a diffracted field contribution must be included to compensate the GO discontinuities. To demonstrate the accuracy of this approximate solution, the results obtained by the PEM (circles) have also been plotted in Fig. 4: an excellent agreement is observed. As expected, the

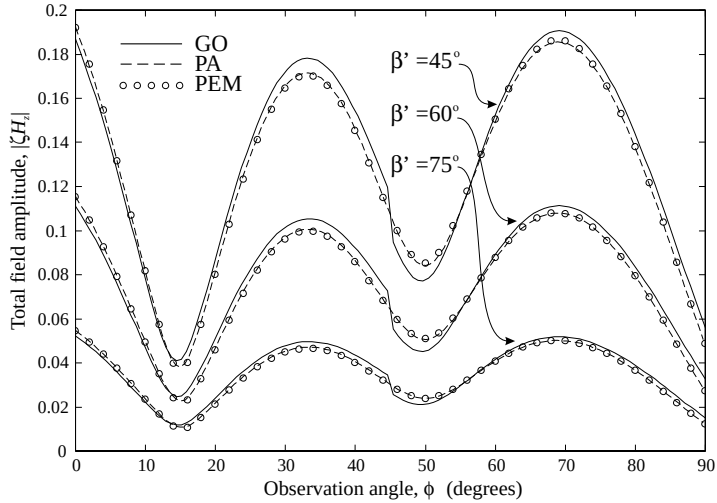

Figure 4. Cross-polar component of the total field (ζH_z) in the presence of an interior right angled anisotropic impedance wedge with $\xi_z^0 = j/2$, $\xi_\rho^0 = j$, $\xi_z^n = (1+j)/2$, $\xi_\rho^n = j$ and $\upsilon = 0.1$. The incident plane wave is TM_z polarized ($e_z^i = 1$, $h_z^i = 0$) and impinges from $\beta' = 45, 60, 75^\circ$ and $\phi' = 45^\circ$. Comparison between our approximate solution including up to the third-order correction (dashed line), the GO solution (continuous line) and the PEM solution (circles).

amplitude of the cross-polar component progressively reduces when the angle β' approaches $\pi/2$, eventually vanishing at normal incidence.

The convergence of the perturbative solution has also been investigated at the increasing of the parameter υ. Data describing the amplitude of the total field scattered from a right-angled wedge illuminated by a TE_z polarized ($e_z^i = 0$, $h_z^i = 1$) plane wave are plotted in Fig. 5; in particular, continuous lines represent this approximate solution while the circles are associated with the results obtained by the parabolic equation method. The wedge is characterized by two anisotropic impedance faces, with $\xi_z^0 = (1 + j/2)/2$, $\xi_\rho^0 = j/2$, $\xi_z^n = (1/2 + j)/2$, $\xi_\rho^n = (2 + 3j)/4$; υ assumes a set of increasing values ($\upsilon = 0.1, 0.2, 0.3$). The plane wave impinges on the edge from $\beta' = 45^\circ$ and $\phi' = 50^\circ$. Several curves, corresponding to the different values of υ, are plotted for both the co-polar (ζH_z) and the cross-polar (E_z) longitudinal components of the total field in Fig. 5(a) and 5(b), respectively. A very good agreement is achieved for small impedances ($\upsilon \leqslant 0.1$). At the increasing of υ, the discrepancy between PA and

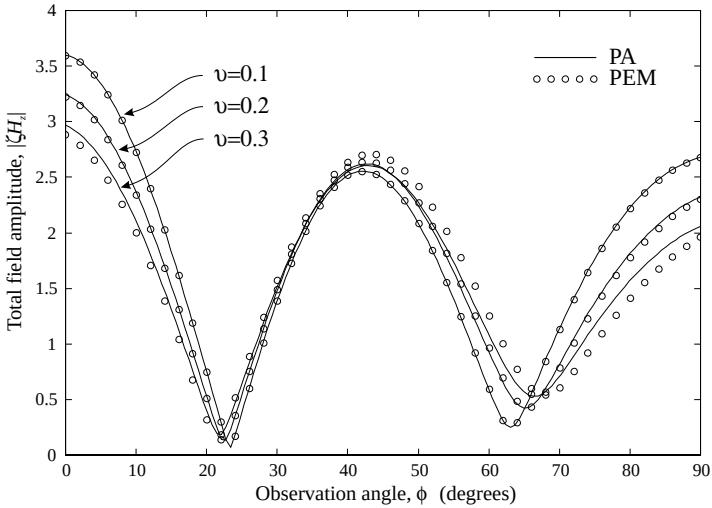

(a)

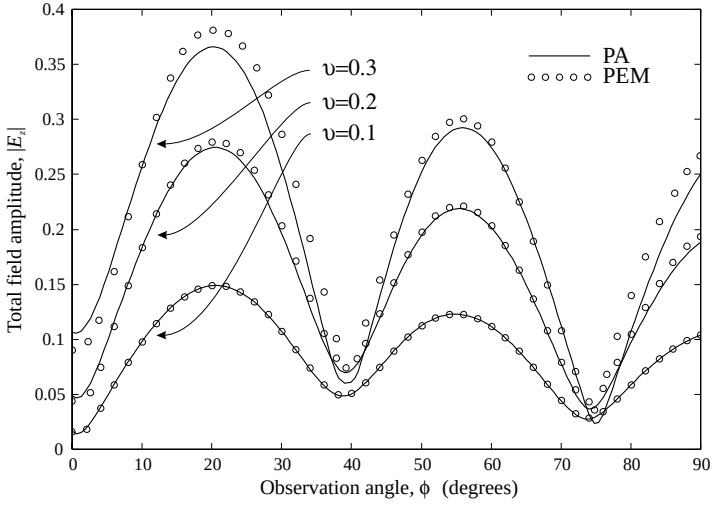

(b)

Figure 5. Total field amplitude in the presence of an interior right angled anisotropic impedance wedge with $\xi_z^0 = (1 + j/2)/2$, $\xi_\rho^0 = j/2$, $\xi_z^n = (1/2 + j)/2$, $\xi_\rho^n = (2 + 3j)/4$, $\upsilon = 0.1, 0.2, 0.3$. The incident plane wave is TE_z polarized ($e_z^i = 0$, $h_z^i = 1$) and impinges from $\beta' = 45°$ and $\phi' = 50°$: (a) co-polar component (ζH_z); (b) cross-polar component (E_z). This approximate solution including up to the third-order correction: continuous line; PEM solution: circles.

PEM results becomes larger, as expected. Nonetheless, it is interesting to note that the perturbative approach shows to be applicable even for not very small values of the surface impedances.

Finally, it has been shown that the proposed approximate high-frequency solution provides accurate results for $\upsilon \leqslant 0.3$, with errors less than a few percent for the co-polar components and less than 10% as far as the cross-polar components are concerned. It is important to underline that the perturbative procedure proposed here does not provide surface wave contributions since the unperturbed configuration, that is the corresponding perfectly conducting wedge, does not allow the propagation of such waves.

6. CONCLUSIONS

The scattering from an interior right-angled wedge with anisotropic impedance faces has been considered. It has been shown that, if the Dybdal compatibility condition is satisfied, the rigorous solution to this problem can be written in terms of the only GO contributions. Then, a perturbative approach, based on the Sommerfeld-Maliuzhinets method, has been developed to estimate the edge diffracted field contribution, when the Dybdal compatibility condition is not satisfied and the normalized surface impedances on the anisotropic faces assume small values. The perturbative corrections to the field have been asymptotically evaluated in the UTD format. Extensive numerical tests have been performed to check the accuracy and the convergence of the perturbative solution through comparisons with reference data obtained by applying the parabolic equation method. Beyond providing a solution for the specific wedge problem under analysis, a further outcome of the paper is that of showing that the Maliuzhinets method can be successfully combined with a perturbative technique to systematically construct an approximate solution for impedance wedge scattering problems. Indeed, as also shown in [13] and [14], once a proper small geometric or electric parameter has been identified and the spectral solution for the corresponding wedge problem with a vanishing value of the above parameter is known (zero-order spectral solution), the perturbative method can be applied to derive inhomogeneous Maliuzhinets' type functional equations for the higher-order terms of the spectral field series representation. The integral solution of the latter functional equations is avalaible in the open literature and can be carried out by resorting to efficient numerical integration techniques.

APPENDIX A. FIRST ORDER SPECTRAL FUNCTIONS

By inserting expressions (19) into Eqs. (18) for $i = 1$, $\left[s_1^e(\alpha), s_1^h(\alpha)\right]$ are found to satisfy the following inhomogeneous functional equations:

$$s_1^e\left(\alpha_{0,n}^+\right) - s_1^e\left(\alpha_{0,n}^-\right) = \frac{A_{0,n}\sin\alpha + \epsilon_{0,n}B_{0,n}\cos\alpha\sin(2\alpha)}{\cos(2\alpha) - \epsilon_{0,n}\cos(2\phi')}, \quad \text{(A1a)}$$

$$s_1^h\left(\alpha_{0,n}^+\right) + s_1^h\left(\alpha_{0,n}^-\right) = \frac{\cos\alpha\left[C_{0,n} - \epsilon_{0,n}\left(D_{0,n} + E_{0,n}\cos^2\alpha\right)\right]}{\cos(2\alpha) - \epsilon_{0,n}\cos(2\phi')}, \quad \text{(A1b)}$$

where $\alpha_{0,n}^+$ and $\epsilon_{0,n}$ have been introduced in the previous sections and

$$\begin{aligned} A_{0,n} &= -4\xi_z^{0,n}\frac{\sin(2\phi')}{\sin\beta'}\, e_z^i, \qquad B_{0,n} = 4\xi_z^{0,n}\cot\beta' h_z^i, \\ C_{0,n} &= 4\xi_z^{0,n}\sin(2\phi')\cot\beta' e_z^i, \quad D_{0,n} = 8\xi_\rho^{0,n}\sin\beta' h_z^i, \\ E_{0,n} &= 8\xi_z^{0,n}\cos\beta'\cot\beta' h_z^i. \end{aligned} \quad \text{(A2)}$$

Due to the linearity of the system in (A1), $s_1^e(\alpha)$ and $s_1^h(\alpha)$ can be written as:

$$\begin{aligned} s_1^e(\alpha) = &\left[A_0\cos\left(\alpha_0^+\right) - B_0\sin\left(\alpha_0^+\right)\cos(2\alpha)\right] f_0(\alpha) \\ &+ \left[A_n\cos\left(\alpha_n^+\right) + B_n\sin\left(\alpha_n^+\right)\cos(2\alpha)\right] f_n(\alpha), \end{aligned} \quad \text{(A3a)}$$

$$\begin{aligned} s_1^h(\alpha) = &-\sin\left(\alpha_0^+\right)\left[C_0 - D_0 + E_0\sin^2\left(\alpha_0^+\right)\right] f_0(\alpha) \\ &+ \sin\left(\alpha_n^+\right)\left[C_n + D_n + E_n\sin^2\left(\alpha_n^+\right)\right] f_n(\alpha). \end{aligned} \quad \text{(A3b)}$$

The functions $f_0(\alpha)$ and $f_n(\alpha)$ must fulfil the following equations

$$\begin{aligned} &f_{0,n}\left(\alpha_{0,n}^+\right) + f_{0,n}\left(\alpha_{0,n}^-\right) = \epsilon_{0,n}\left[\cos(2\alpha) - \epsilon_{0,n}\cos\left(2\phi'\right)\right]^{-1} \\ &f_{0,n}\left(\alpha_{n,0}^+\right) - f_{0,n}\left(\alpha_{n,0}^-\right) = 0, \end{aligned} \quad \text{(A4)}$$

whose solutions can be conveniently derived in terms of modified Fourier integrals as in [21, 23]:

$$f_{0,n}(\alpha) = \left\{\int_{-\sigma-j\infty}^{-\sigma+j\infty} + \int_{\sigma-j\infty}^{\sigma+j\infty}\right\} \frac{j\sin\left[\omega\left(\phi_{n,0}\right)\right] e^{-j\omega\left(\alpha - \epsilon_{0,n}\frac{\pi}{4}\right)}}{4\sin(\omega\pi)\sin(2\phi')} d\omega, \quad \text{(A5)}$$

where σ is greater than zero and sufficiently small. By exploiting the following relationship [21]

$$t\left(\alpha-\pi,\phi'\right)-t\left(\alpha+\pi,\phi'\right)=\left(\cos\alpha-\cos\phi'\right)^{-1}, \tag{A6}$$

where

$$t\left(\alpha,\phi'\right)=\frac{1}{4\sin\left(\pi-\phi'\right)}\left\{\int_{-\sigma-j\infty}^{-\sigma+j\infty}+\int_{\sigma-j\infty}^{\sigma+j\infty}\right\}\frac{\sin\left[\omega\left(\phi'-\pi\right)\right]e^{-j\omega\alpha}}{\sin^2\left(\omega\pi\right)}d\omega, \tag{A7}$$

$f_0(\alpha)$ and $f_n(\alpha)$ can be expressed in a closed form:

$$f_{0,n}\left(\alpha\right)=\frac{\epsilon_{0,n}\,\cos\left(\phi_{0,n}\right)}{2\sin(2\phi')\left[\cos\left(\alpha_{0,n}^{+}\right)+\epsilon_{0,n}\,\sin\left(\phi_{0,n}\right)\right]}. \tag{A8}$$

By substituting (A2) and (A8) into (A3), complete expressions for the first order correction spectral functions $\left[s_1^e(\alpha),s_1^h(\alpha)\right]$ are obtained.

APPENDIX B. SECOND ORDER SPECTRAL FUNCTIONS

The functional equations holding for $s_2^e(\alpha)$ and $s_2^h(\alpha)$ can be obtained by inserting the explicit expressions for $\left[s_1^e(\alpha),s_1^h(\alpha)\right]$ into Eqs. (18) for $i=2$. The spectra $\left[s_2^e(\alpha),s_2^h(\alpha)\right]$ can be written as:

$$s_2^e(\alpha)=\overline{s}_2^{\,e}(\alpha)+\widehat{s}_2^{\,e}(\alpha), \tag{B1a}$$

$$s_2^h(\alpha)=\overline{s}_2^{\,h}(\alpha)+\widehat{s}_2^{\,h}(\alpha). \tag{B1b}$$

In (B1), $\overline{s}_2^{\,e}(\alpha)$ and $\overline{s}_2^{\,h}(\alpha)$ must satisfy the following equations:

$$\begin{aligned}\overline{s}_2^{\,e}\left(\alpha_{0,n}^{+}\right)-\overline{s}_2^{\,e}\left(\alpha_{0,n}^{-}\right)&=\frac{\sin\alpha\left[L_{0,n}^1\sin^2\alpha+L_{0,n}^2\sin^2\left(2\alpha\right)\right]}{\cos\left(2\alpha\right)-\epsilon_{0,n}\cos\left(2\phi'\right)}\\&\quad+\frac{\sin\alpha\left(L_{0,n}^3\cos^2\alpha+L_{0,n}^4\cos^4\alpha\right)}{\cos\left(2\alpha\right)-\epsilon_{0,n}\cos\left(2\phi'\right)},\end{aligned} \tag{B2a}$$

$$\begin{aligned}\overline{s}_2^{\,h}\left(\alpha_{0,n}^{+}\right)+\overline{s}_2^{\,h}\left(\alpha_{0,n}^{-}\right)&=\frac{\cos\alpha\left(M_{0,n}^1+M_{0,n}^2\cos^2\alpha+M_{0,n}^3\cos^4\alpha\right)}{\cos\left(2\alpha\right)-\epsilon_{0,n}\cos\left(2\phi'\right)}\\&\quad+\frac{\cos\alpha\left[M_{0,n}^4\sin^2\alpha+M_{0,n}^5\sin^2\left(2\alpha\right)\right]}{\cos\left(2\alpha\right)-\epsilon_{0,n}\cos\left(2\phi'\right)},\end{aligned} \tag{B2b}$$

where we have set

$$
\begin{aligned}
L^1_{0,n} &= \frac{8\left(\xi_z^{0,n}\right)^2 \cos\left(\phi_{0,n}\right)\, e_z^i}{\sin^2\beta'}, \quad L^2_{0,n} = -\frac{2\left(\xi_z^{0,n}\right)^2 \cos\beta'\, h_z^i}{\sin^2\beta' \sin\left(\phi_{0,n}\right)}, \\
L^3_{0,n} &= L^1_{0,n}\cos^2\beta' + 4L^2_{0,n}\frac{\xi_\rho^{0,n}}{\xi_z^{0,n}}\sin^2\beta', \quad L^4_{0,n} = 4L^2_{0,n}\cos^2\beta', \\
M^1_{0,n} &= \frac{8\left(\xi_\rho^{0,n}\right)^2 \sin^2\beta'\, h_z^i}{\sin\left(\phi_{0,n}\right)} - 8\xi_\rho^{0,n}\xi_z^{0,n}\cos\beta'\cos\left(\phi_{0,n}\right), \\
M^2_{0,n} &= M^1_{0,n}\cot^2\beta'\frac{\xi_z^{0,n}}{\xi_\rho^{0,n}} + \frac{8\xi_z^{0,n}\xi_\rho^{0,n}\cos^2\beta'\, h_z^i}{\sin\left(\phi_{0,n}\right)}, \\
M^3_{0,n} &= -L^4_{0,n}\cos\beta', \; M^4_{0,n} = -L^1_{0,n}\cos\beta', \; M^5_{0,n} = -L^2_{0,n}\cos\beta'.
\end{aligned}
\tag{B3}
$$

Since Eqs. (B2) are of the same type as those in (A1), by using the same procedure outlined in Appendix A, the spectral functions $\overline{s}_2^{\,e}(\alpha)$ and $\overline{s}_2^{\,h}(\alpha)$ can be expressed in terms of $f_0(\alpha)$ and $f_n(\alpha)$, given by Eq. (A8), as follows:

$$
\begin{aligned}
\overline{s}_2^{\,e}(\alpha) = &\left\{\cos\left(\alpha_0^+\right)\left[L_0^1\cos^2\left(\alpha_0^+\right) + L_0^2\cos^2\left(2\alpha\right)\right] + \right. \\
&-\sin\left(\alpha_0^+\right)\cos\left(2\alpha\right)\left[L_0^3 + L_0^4\sin^2\left(\alpha_0^+\right)\right]/2\Big\} f_0(\alpha) \\
&+\left\{\cos\left(\alpha_n^+\right)\left[L_n^1\cos^2\left(\alpha_n^+\right) + L_n^2\cos^2\left(2\alpha\right)\right]\right. \\
&\left.+\sin\left(\alpha_0^+\right)\cos\left(2\alpha\right)\left[L_n^3 + L_n^4\sin^2\left(\alpha_n^+\right)\right]/2\right\} f_n(\alpha),
\end{aligned}
\tag{B4a}
$$

$$
\begin{aligned}
\overline{s}_2^{\,h}(\alpha) = &-\left[M_0^1 + M_0^2\sin^2\left(\alpha_0^+\right) + M_0^3\sin^4\left(\alpha_0^+\right)\right. \\
&\left.+\, M_0^4\cos^2\left(\alpha_0^+\right) + M_0^5\cos^2\left(2\alpha\right)\right]\sin\left(\alpha_0^+\right) f_0(\alpha) \\
&+\left[M_n^1 + M_n^2\sin^2\left(\alpha_n^+\right) + M_n^3\sin^4\left(\alpha_n^+\right)\right. \\
&\left.+\, M_n^4\cos^2\left(\alpha_n^+\right) + M_n^5\cos^2\left(2\alpha\right)\right]\sin\left(\alpha_n^+\right) f_n(\alpha).
\end{aligned}
\tag{B4b}
$$

As far as $\widehat{s}_2^{\,e}(\alpha)$ and $\widehat{s}_2^{\,h}(\alpha)$ in Eq. (B1) are concerned, the functional equations to be solved are:

$$
\widehat{s}_2^{\,e}\left(\alpha_{0,n}^+\right) - \widehat{s}_2^{\,e}\left(\alpha_{0,n}^-\right) = \frac{\sin\alpha\cos\alpha\left(L_{0,n}^5 + L_{0,n}^6\sin^2\alpha\right)}{\cos\alpha + \cos\left(\phi_{0,n}\right)}, \tag{B5a}
$$

$$
\widehat{s}_2^{\,h}\left(\alpha_{0,n}^+\right) + \widehat{s}_2^{\,h}\left(\alpha_{0,n}^-\right) = \frac{\left[M_{0,n}^6 + M_{0,n}^7\sin^2\alpha + M_{0,n}^8\sin^2\left(2\alpha\right)\right]}{\cos\alpha + \cos\left(\phi_{0,n}\right)}, \tag{B5b}
$$

where we have defined

$$
\begin{aligned}
L^5_{0,n} &= 4\epsilon_{0,n}\,\xi^0_z\xi^n_z \sin(\phi_{0,n})\, e^i_z - \frac{4\epsilon_{0,n}\,\xi^{0,n}_z\xi^{n,0}_\rho \cos\beta'\, h^i_z}{\cos(\phi_{0,n})},\\
L^6_{0,n} &= \frac{4\,\epsilon_{0,n}\,\xi^0_z\,\xi^n_z \cos\beta'\, h^i_z}{\cos(\phi_{0,n})},\\
M^6_{0,n} &= \cos\beta'\big[4\epsilon_{0,n}\,\xi^{0,n}_\rho\xi^{n,0}_z \sin(\phi_{0,n})\, e^i_z - L^5_{0,n}\big] + \frac{4\,\epsilon_{0,n}\,\xi^0_\rho\,\xi^n_\rho \sin^2\beta' h^i_z}{\cos(\phi_{0,n})},\\
M^7_{0,n} &= L^5_{0,n}\cos\beta' + \epsilon_{0,n}L^6_{0,n}\cos\beta'\frac{\xi^0_\rho}{\xi^0_z}, \quad M^8_{0,n} = -\frac{L^6_{0,n}}{4}\cos\beta'.
\end{aligned}
\tag{B6}
$$

Solutions to the equations in (B5), which are similar to those in (A1) and (B2), can be obtained by representing $\widehat{s}^{\,e}_2(\alpha)$ and $\widehat{s}^{\,h}_2(\alpha)$ as follows:

$$
\begin{aligned}
\widehat{s}^{\,e}_2(\alpha) =& \sin\left(\alpha^+_0\right)\cos\left(\alpha^+_0\right)\left[L^5_0 + L^6_0\cos^2\left(\alpha^+_0\right)\right] g_0(\alpha)\\
&+ \sin\left(\alpha^+_n\right)\cos\left(\alpha^+_n\right) + \left[L^5_n + L^6_n\cos^2\left(\alpha^+_n\right)\right] g_n(\alpha),
\end{aligned}
\tag{B7a}
$$

$$
\begin{aligned}
\widehat{s}^{\,h}_2(\alpha) =& -\left[M^6_0 + M^7_0\cos^2\left(\alpha^+_0\right) + M^8_0\cos^2(2\alpha)\right] g_0(\alpha) +\\
&- \left[M^6_n + M^7_n\cos^2\left(\alpha^+_n\right) + M^8_n\cos^2(2\alpha)\right] g_n(\alpha).
\end{aligned}
\tag{B7b}
$$

Insertion of (B7) into (B5) yields the following system of functional equations for $g_0(\alpha)$ and $g_n(\alpha)$:

$$
\begin{aligned}
&g_{0,n}\left(\alpha^+_{0,n}\right) + g_{0,n}\left(\alpha^-_{0,n}\right) = -\left[\cos\alpha + \cos(\phi_{0,n})\right]^{-1},\\
&g_{0,n}\left(\alpha^+_{n,0}\right) + g_{0,n}\left(\alpha^-_{n,0}\right) = 0.
\end{aligned}
\tag{B8}
$$

Through the application of the Fourier transform [21], suitable integral representations for $g_0(\alpha)$ and $g_n(\alpha)$ can be obtained:

$$
g_{0,n}(\alpha) = \left\{\int_{-\sigma-j\infty}^{-\sigma+j\infty} + \int_{\sigma-j\infty}^{\sigma+j\infty}\right\} \frac{\epsilon_{0,n}\,\sin\left[\omega(\phi_{0,n})\right] e^{-j\omega\left(\alpha-\epsilon_{0,n}\frac{\pi}{4}\right)}}{4\sin(\phi_{0,n})\sin(\omega\pi)\sin(\omega\pi/2)}\, d\omega.
\tag{B9}
$$

By observing that for the function $t(\alpha,\phi')$, which has been previously introduced in Eq. (A7), holds the identity [23]

$$
t(\alpha,\phi') = \frac{\alpha\sin\phi' - (\pi-\phi')\sin\alpha}{2\pi\sin\phi'(\cos\alpha+\cos\phi')},
\tag{B10}
$$

and by also noting that

$$\frac{\sin(\omega v)}{\sin(\omega\pi)\sin(\omega\pi/2)} = \frac{\sin[\omega(v+\pi/2)] + \sin[\omega(v-\pi/2)]}{\sin^2(\omega\pi)}, \tag{B11}$$

we can explicitly rewrite $g_0(\alpha)$ and $g_n(\alpha)$ in the following form:

$$\begin{aligned} g_{0,n}(\alpha) = {} & \frac{\epsilon_{0,n}\ (\phi_{0,n}) \sin\left(2\alpha_{0,n}^{+}\right)}{2\pi \sin(\phi_{0,n}) \left[\cos^2\left(\alpha_{0,n}^{+}\right) - \sin^2(\phi_{0,n})\right]} \\ & + \epsilon_{0,n} \frac{2\left(\alpha_{0,n}^{+}\right)\cos(\phi_{0,n}) - \pi \sin\left(\alpha_{0,n}^{+}\right)}{2\pi\left[\cos^2\left(\alpha_{0,n}^{+}\right) - \sin^2(\phi_{0,n})\right]}. \end{aligned} \tag{B12}$$

Insertion of (B4) and (B7) together with (A8) and (B12) into (B1) yields the complete closed form expressions for $s_2^e(\alpha)$ and $s_2^h(\alpha)$.

REFERENCES

1. Kildal, P. S., A. A. Kishk, and A. Tengs, "Reduction of forward scattering from cylindrical objects using hard surfaces," *IEEE Trans. Antennas and Propagat.*, Vol. 44, 1509–1520, Nov. 1996.
2. Michelson, D. G. and E. V. Jull, "Depolarizing trihedral corner reflectors for radar navigation and remote sensing," *IEEE Trans. Antennas Propagat.*, Vol. 43, 513–518, May 1995.
3. Gennarelli, C., G. Pelosi, and G. Riccio, "Physical optics analysis of the field backscattered by a depolarizing trihedral corner reflector," *IEE Proc.—Microwave, Antennas Propagat.*, Vol. 145, 213–218, June 1998.
4. Senior, T. B. A. and J. L. Volakis, *Approximate Boundary Conditions in Electromagnetics*, IEE Press, Stevenage, U.K., 1995.
5. Manara, G., P. Nepa, and G. Pelosi, "High-frequency EM scattering by edges in artificially hard and soft surfaces illuminated at oblique incidence," *IEEE Trans. Antennas Propagat.*, Vol. 48, 790–800, May 2000.
6. Bilow, H. J., "Scattering by an infinite wedge with tensor impedance boundary conditions—a moment method/physical optics solution for the currents," *IEEE Trans. Antennas Propagat.*, Vol. 39, 767–773, June 1991.
7. Maliuzhinets, G. D., "Developments in our concepts of diffraction phenomena," *Sov. Phys.: Usp.*, Vol. 69(2), No. 5, 749–758, 1959.

8. Popov, A. V., "Numerical solution of the wedge diffraction problem by the transverse diffusion," *Sov. Phys. Acoust.*, Vol. 15, No. 2, 226–233, Oct.–Dec. 1969.
9. Pelosi, G., S. Selleri, and R. D. Graglia, "The parabolic equation model for the numerical analysis of the diffraction at an impedance wedge: skew incidence case," *IEEE Trans. Antennas Propagat.*, Vol. 44, 267–268, 1996.
10. Zhu, N. Y. and F. M. Landstofer, "Numerical study of diffraction and slope-diffraction at anisotropic impedance wedges by the method of parabolic equation: space wave," *IEEE Trans. Antennas Propagat.*, Vol. 45, 822–828, 1997.
11. Nefedov, Y. I. and A. T. Fialkovskiy, "Diffraction of plane electromagnetic wave at anisotropic half-plane in free space and in planar waveguide," *Radio Eng. Electron. Physics*, Vol. 17, No. 6, 887–896, 1972.
12. Lyalinov, M. A., "Diffraction by a wedge with anisotropic face impedances," *Ann. Télécommun.*, Vol. 49, 667–672, Nov.–Dec. 1994.
13. Pelosi, G., G. Manara, and P. Nepa, "Diffraction by a wedge with variable-impedance walls," *IEEE Trans. Antennas Propagat.*, Vol. 44, 1334–1340, Oct. 1996.
14. ——, "A UTD solution for the scattering by a wedge with anisotropic impedance faces: skew incidence cases," *IEEE Trans. Antennas Propagat.*, Vol. 46, 579–588, April 1998.
15. Senior, T. B. A., "Skew incidence on a right-angled wedge," *Radio Sci.*, Vol. 13, No. 4, 639–647, Jul.–Aug. 1978.
16. Dybdal, R., L. Peters, Jr., and W. Peake, "Rectangular waveguides with impedances walls," *IEEE Trans. Microwave Theory Tech.*, Vol. 19, 2–9, 1971.
17. Maliuzhinets, G. D., "Excitation, reflection and emission of surface waves from a wedge with given face impedances," *Sov. Phys. Dokl.*, Vol. 3, 752–755, 1958.
18. Kouyoumjian, R. G. and P. H. Pathak, "A uniform geometrical theory of diffraction for an edge in a perfectly conducting surface," *Proc. IEEE*, Vol. 62, No. 11, 1448–1461, Nov. 1974.
19. Maliuzhinets, G. D., "Inversion formula for the Sommerfeld integral," *Sov. Phys. Dokl.*, Vol. 3, 52–56, 1958.
20. Bowman, J. J. and T. B. A. Senior, "The wedges," *Electromagnetic and Acoustic Scattering by Simple Shapes*, J. J. Bowman, T. B. A. Senior, and P. L. E. Uslenghi (Eds.), 252–283, North-Holland, Amsterdam, 1969.

21. Maliuzhinets, G. D., "The radiation of sound by the vibrating boundaries of an arbitrary wedge. Part I," *Sov. Phys. Acoust.*, Vol. 1, 152–174, 1955.
22. Tuzhilin, A. A., "The theory of Maliuzhinets inhomogeneous functional equations," *Differ. Urav.*, Vol. 9, 2058–2064, 1973.
23. Maliuzhinets, G. D., "Radiation of sound from the vibrating faces of an arbitrary wedge. Part II," *Sov. Phys. Acoust.*, Vol. 1, 240–248, 1955.

Giuliano Manara was born in Florence, Italy, on October 30, 1954. He received the Laurea (Doctor) degree in electronics engineering (*summa cum laude*) from the University of Florence, Italy, in 1979. He was first with the Department of Electronic Engineering, University of Florence, as a Postdoctoral Research Fellow. Then, in 1987, he joined the Department of Information Engineering, University of Pisa, where he works presently as a Full Professor. Since 1980, he has been collaborating with the Department of Electrical Engineering, Ohio State University, Columbus, where in summer and fall of 1987 he was involved in research at the ElectroScience Laboratory. His current research interests include radar systems, numerical and asymptotic techniques in electromagnetic scattering, and radiation problems. Dr. Manara is a senior member of IEEE.

Paolo Nepa received the Laurea (Doctor) degree in electronics engineering (summa cum laude) from the University of Pisa, Italy, in 1990. Since 1990, he has been with the Department of Information Engineering, University of Pisa, where he is currently an Associate Professor. In 1998, he was at the ElectroScience Laboratory (ESL), The Ohio State University (OSU), Columbus, OH, as a Visiting Scholar supported by a grant of the Italian National Research Council. His research interests include the extension of high-frequency techniques to electromagnetic scattering from material structures and the design of base station antennas for wireless communication systems.

Giuseppe Pelosi was born in Pisa, Italy, on December 25, 1952. He received the Laurea (Doctor) degree in physics (summa cum laude) from the University of Florence in 1976. Since 1979, he is with the Department of Electronic Engineering of the University of Florence, where he is currently a Full Professor of Electromagnetic Fields. He has been visiting scientist at the McGill University, Montreal, PQ, Canada. G. Pelosi has been mainly involved in research in the field of numerical and asymptotic techniques for applied electromagnetics. His current

research activity is mainly devoted to the development of numerical procedures in the context of the Finite Element Method, with particular emphasis on radiation and scattering problems. He is author of three books, "Finite Elements for Wave Electromagnetics" (IEEE Press, 1994), "Finite Element Software for Microwave Engineering" (John Wiley, 1996) and "Quick Finite Element for Electromagnetic waves" (Artech House, 1998). Dr. Pelosi is Fellow of IEEE and Member of the Applied Computational Electromagnetics Society.

Andrea Vallecchi graduated (cum laude) in Electronic Engineering from the University of Florence, Italy, in 1998 and received his Ph.D. degree in Applied Electromagnetics from the University of Salerno, Italy, in 2002. He is currently a research associate at the Laboratory of Antennas and Microwaves of the University of Florence. His research activity is mainly concerned with the development and application of uniform asymptotic techniques in electromagnetic scattering from complex imperfectly reflecting bodies and the analysis and design of microstrip antennas and arrays.